J Fluoresc (2012) 22:289–301
DOI 10.1007/s10895-011-0959-3

ORIGINAL PAPER

Modulation of Intramolecular Charge Transfer Emission Inside Micelles: A Fluorescence Probe for Studying Microenvironment of Micellar Assemblies

Anuva Samanta · Bijan Kumar Paul · Nikhil Guchhait

Received: 24 June 2011 / Accepted: 30 August 2011 / Published online: 9 September 2011

Abstract Modulation of intramolecular charge transfer reaction of ethyl ester of N,N-Dimethylaminonaphthyl-(acrylic)-acid (EDMANA) in anionic sodium dodecyl sulfate (SDS), cationic cetyltrimethylammonium bromide (CTAB) and non-ionic *p-tert*-octylphenoxy polyoxyethanol (Triton-X 100, TX-100) micelles has been addressed using steady state and time resolved spectroscopy. The interaction of the CT probe EDMANA with micelles and its location inside the micelles have been investigated by the study of fluorescence spectral band position of EDMANA in micelle, the effective polarity of micelle-water interface and cetyl pyridinium chloride induced fluorescence quenching measurement. The effects of urea on the properties of the micelles such as Critical Micelle Concentration and the interaction between EDMANA and micelles have been explored using EDMANA as emission probe.

Keywords Micelle · N,N-Dimethylaminonaphthyl-(acrylic)-acid ethyl ester · Fluorescence · Charge transfer · Critical micelle concentration (CMC) · Urea

Introduction

Since Lippert's first report [1], one of the most extensively studied example of excited state charge transfer process is the dual fluorescence of 4-(N,N-Dimethylamino)benzonitrile (DMABN) [2–9]. Molecules with a flexible single bond between the donor and acceptor subunit are capable to rotate around the bond, thereby stabilizing the intramolecular charge transfer (ICT) state in solvents of higher dielectric. It has been well accepted [10–14] that dual fluorescence arises due to equilibrium between two states in the excited state surface. The short wavelength emission (b*) band is due to a coplanar structure of the molecule, while the "abnormal" long wavelength emission (a*) band originates from a structure with a perpendicular conformation which under appropriate conditions can be preferentially stabilized having much higher dipole moment than that of its precursor locally excited (LE) state. The high dipole moment of the fluorescent charge transfer (CT) state makes the fluorophore very useful in probing both the bulk and microenvironments of different media, such as supercritical fluids [15, 16], cyclodextrins [17–19] and micelles [20–23]. The advantage behind the use of CT molecule as fluoro-probe is based on the medium dependent spectral properties of the generated CT state.

Research on micellar media is very important due to their microenvironmental similarity with proteins, enzymes etc., their biomimicking nature and capability of some of them to efficiently accommodate and transport of drugs [24–28]. The most significant property of an organized assembly of nano dimensions is its ability to stabilize and bind solute molecules that are typically insoluble or sparingly soluble in a pure bulk solvent. Upon binding a molecule will experience a different environment inside the microheterogeneous structure of micelle than that of the bulk solvents. Properties like polarity, steric rigidity, viscosity and diffusion of water molecules towards the core of the micelle are different from the bulk phase [23]. Micelles are characterized by two regions, a hydrophobic core and a hydrophilic surface that may be cationic, anionic

A. Samanta · B. K. Paul · N. Guchhait (✉)
Department of Chemistry, University of Calcutta,
92 A. P. C. Road,
Kolkata 700009, India
e-mail: nguchhait@yahoo.com

and non-ionic. All these three types of micelles consist of a dry hydrocarbon core surrounded by a wet spherical shell called the Stern layer with thickness 6–10 Å for ionic micelle and 25 Å for palisade layer of non-ionic micelle. Surrounding the Stern layer is a diffuse layer called the Gouy Chapman layer. This outer layer is about several hundred angstroms wide [28]. The ionic micelle consists of a micelle-water interface and the charge of this interface can be modulated by the embodiment of sensor molecules or ions. With the introduction of a proper fluorescent probe that is very sensitive to environmental polarity and viscosity, one can follow the process of micellization and also the effect of interface electric field on the probe. Therefore, structural study of different micelles and their influence on photoinduced processes are fascinating and have been discussed in several reviews [26, 27, 29, 30].

In our previous work [31], we have reported that the fluorescence properties of ethyl ester of N,N-Dimethylaminonaphthyl-(acrylic)-acid (EDMANA) is very much dependent on the solvent polarity. In particularly, the fluorescence maxima shifts to the red with increasing solvent polarity and fluorescence quantum yield changes with viscosity and hydrogen bonding ability of the solvent. Since micelles contain hydrophobic and hydrophilic regions with confined cage, it would be interesting to study the photophysics of EDMANA in the micellar nanocage. Considering the polarity sensing ability of EDMANA, we thought that this molecule would provide information on the local polarity of the micelle environment. Therefore, in the present work, we have studied the micellization process of non-ionic (Triton-X 100, TX-100), anionic (sodium dodecyl sulfate, SDS) and cationic (cetyltrimethylammonium bromide, CTAB) micelles using EDMANA as an external fluorescence probe by steady state and time resolved spectroscopy. The chaotrope urea has the denaturation tendency to protein and inhibition criteria on micellization process due to its ability to weaken of hydrophobic forces in aqueous solution [32–35]. Since micelles are relatively simple models for more complex biological systems, a number of recent studies have been undertaken to elucidate the action of urea on it [32–35]. From these investigations, it has been found that urea increases the Critical Micelle Concentration (CMC) of ionic [32, 33, 35] and non-ionic surfactants [33, 34]. We have studied the emission properties of probe EDMANA to study the effect of urea on the properties of micelles and on the interaction between probe and micelles.

Experimental Section

The synthetic procedure of EDMANA (Scheme 1) has been described in our previous publication [31]. The surfactants SDS, CTAB and TX-100 (Scheme 1) were purchased from SRL, Spectrochem and Merck, respectively, and used as supplied. Triply distilled water was used for preparing solutions. Methanol and 1,4-dioxane from Spectrochem and glycerol from Merck were used as supplied. Analytical grade urea (Merck) and cetyl pyridinium chloride (CPCL) from Loba Chemie were used in this work.

The absorption and emission spectra of EDMANA in different medium have been taken by Hitachi UV–vis (Model U-3501) spectrophotometer and PerkinElmer (Model LS-55) fluorimeter, respectively In all measurements, the sample concentration has been maintained within the range 10^{-5}–10^{-6} mol/dm^3 in order to avoid dimerization.

The time resolved fluorescence intensity decays were obtained with a Time Correlated Single Photon Counting

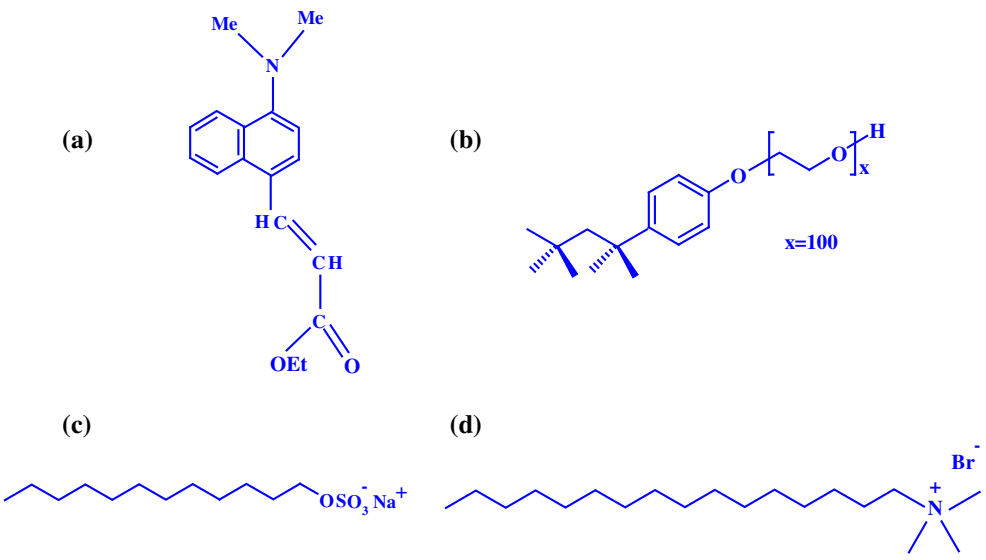

Scheme 1 Structure of **a** ethyl ester of N,N′-Dimethylamino-naphthyl-(acrylic)-acid (EDMANA) **b** TX-100, **c** SDS and **d** CTAB

(TCSPC) set up employing a nanosecond diode laser (IBH, nanoLED-07) operating at λ_{ex}=340 nm as the light source (FWHM=900 ps) and TBX-04 as the detector [36]. The fluorescence decay was collected with an emission polarizer kept at the magic angle (~54.7^0). The decays were analyzed using Data Station v-2.5 decay analysis software. Intensity decay curves were obtained as a sum of exponential terms

$$F(t) = \sum_i a_i \exp\left(\frac{-t}{\tau_i}\right) \quad (1)$$

Where F(t) is the fluorescence intensity at time t, a_i the pre-exponential factor representing the fractional contribution to the time resolved decay of the i^{th} component with a lifetime τ_i. Average lifetimes (τ_{avg}) of fluorescence were calculated from the decay times and pre-exponential factors using the following equation:

$$\tau_{avg} = \sum_i a_i \tau_i \quad (2)$$

The fluorescence quantum yields were estimated from the corrected fluorescence spectra using quinine sulphate in 0.1 M H_2SO_4 (Φ_F=0.577 at 293 K) as standard [37].

Results and Discussion

Absorption Study

The absorption and emission spectra of EDMANA in different solvents have been elaborately discussed in our previous publication [31]. In brief the molecule shows its ππ* absorption for the naphthalene chromophore at 352 nm in aqueous solution. Absorption spectra of EDMANA in an aqueous solution with varying concentration of three different surfactants (SDS, CTAB and TX-100) have been recorded keeping the concentration of EDMANA fixed in each case (Fig. 1) and the relevant spectral data are presented in Table 1. From Fig. 1, it is clear that with increasing of surfactant concentration the ππ* absorption band of EDMANA is red shifted by 6–10 nm in ionic micelles with concurrent increase in absorbance whereas addition of neutral TX-100 micelle causes a slight enhancement of that band intensity only (Fig. 1c). The increase in absorbance in each micelle compared to bulk medium may be attributed to enhanced solubilization of EDMANA in micelle solution. It is noteworthy to mention here that EDMANA forms hydrogen bonded cluster in water and hence absorption band is shifted to blue in water compared to other aprotic solvents [31]. Therefore, the apparent red shift may indicate the movement of the molecule from pure aqueous phase to micellar less polar environment.

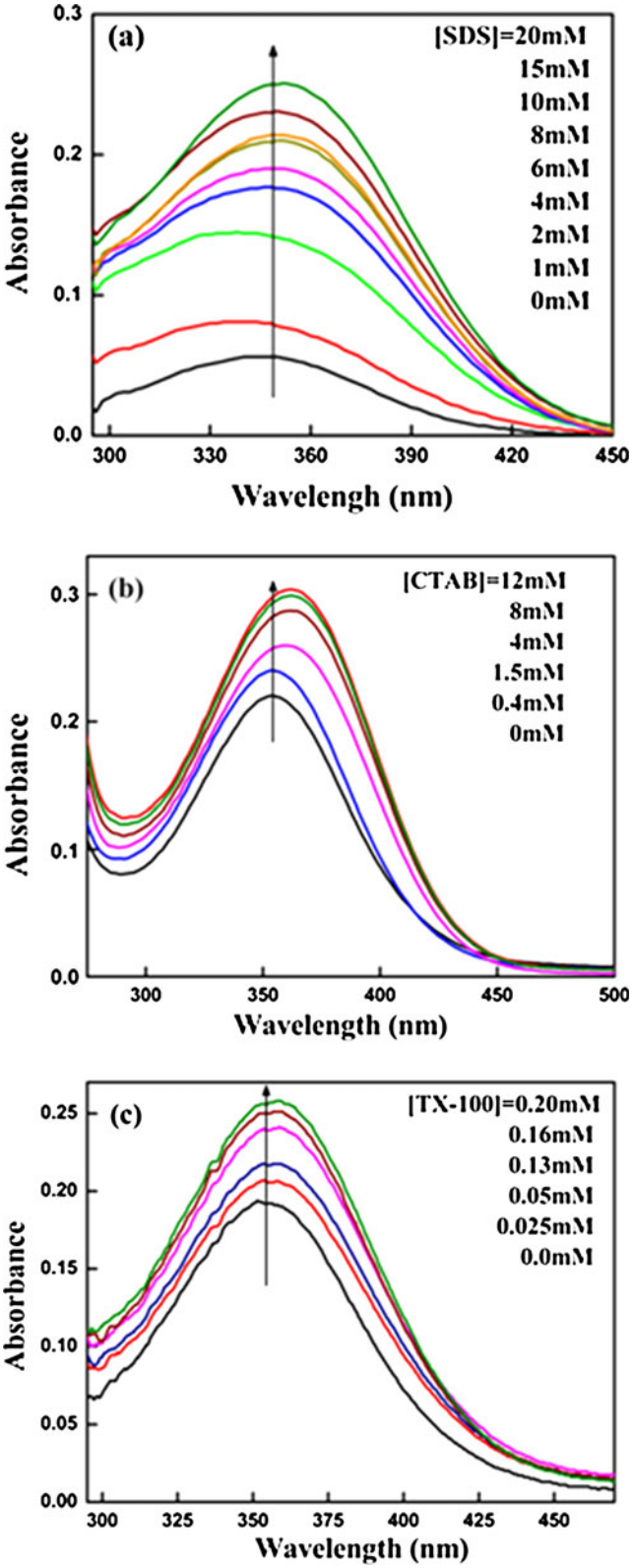

Fig. 1 UV-visible absorption spectra of EDMANA in aqueous solution with varying concentration of **a** SDS, **b** CTAB and **c** TX-100 at room temperature

Table 1 UV–vis absorption and fluorescence band maxima, fluorescence quantum yield, binding constants and free energy change of EDMANA in different micelles at room temperature

Solvent/Medium	λ_a (nm)	λ_f (nm)	Φ_F (x10^3)	K_{eq} (x10^{-5} M^{-1})	ΔG^0 (kJ/mol)
Water	352	521	7.84	–	–
SDS	358	504	30.0	0.89±0.02	−28.42
CTAB	362	498	41.3	4.36±0.48	−32.39
TX-100	356	492	44.2	7.63±0.67	−33.78

Fluorescence Emission Study

Fluorescence techniques have been widely used to characterize micellar organization and dynamics due to their intrinsic sensitivity and suitable time scale [38]. The present molecule EDMANA having donor and acceptor group capable for charge transfer reaction in the excited state shows solvent polarity dependent red shifted CT emission in addition to the high energy local emission [31]. Interestingly the emission spectral parameters such as fluorescence intensity, quantum yield and fluorescence lifetime of the CT state of EDMANA are found to be affected by the nature of the solvent [31]. The observed fluorescence properties are found to be low in protic solvents compared to the aprotic solvents due to non-radiative deactivation by intermolecular hydrogen bonding interaction. The excited state behavior of EDMANA in different micelles has been studied and the corresponding emission spectra are depicted in Fig. 2. The molecule shows its emission at 521 nm in pure water. An enhancement of the fluorescence intensity with blue shift (17 nm in SDS, 23 nm in CTAB and 29 nm in TX-100) has been observed on gradual addition of SDS, CTAB and TX-100 in aqueous solution of EDMANA (Table 1). Both observations reflect that microenvironment around the fluorophore is the micellar assemblies being quite different from those in the pure aqueous phase. The spectral shifts and the enhancement of the fluorescence intensities can be explained in terms of binding of this probe to a less polar site of the micelle. It is already known that EDMANA undergoes photoinduced ICT reaction; therefore reduced polarity does not stabilize the excited state more than the ground state. As a result, the energy gap between this state and the ground state increases showing blue shifting in the emission maxima. As seen in Table 1, the fluorescence quantum yield of the CT band increases appreciably as the fluorophore is trapped in the micellar environment. Enhancement of red shifted CT emission may infer that confined micellar nanocage may enhance charge transfer reaction and reduces non-radiative deactivation channels. It is noteworthy to mention here that excited state CT reaction favors in more polar solvent. The trend in increasing fluorescence intensity and quantum yield of CT emission of EDMANA with decreasing polarity of the micellar cage in the order of SDS<CTAB<TX-100 indicate that micellar nanocage mainly deactivates the non-radiative channels but not the CT reaction in the excited state. Later on we have found that strong binding constant and viscosity trend in the order of TX-100>CTAB>SDS are responsible for increasing fluorescence intensity and quantum yield. Different extent of blue shifts, enhancement of CT bands and fluorescence quantum yields in three micelles surely point that the location of the emitting species is not same in all these micelles.

Time Resolved Studies

Fluorescence lifetime serves as a sensitive indicator of the local environment in which a given fluorophore is placed. So this technique could provide valuable information regarding the location and distribution of a probe in complex microheterogeneous environments such as protein, micelle, lipid etc. in a better way. So modulated photophysics of EDMANA in micellar environment compared to aqueous media has been demonstrated using time resolved study. The lifetime of EDMANA in aqueous solution can not be obtained due to its ultrafast decay nature that is below the resolution limit (90 ps) of the lifetime instrument. Typical decay profiles of EDMANA in micellar media are shown in Fig. 3 and the corresponding lifetime data are tabulated in Table 2. Single and bi-exponential fitting of the decay profiles have been done in order to get acceptable χ^2 values though the pre-exponential value of the long-lived component is too small. As shown in Table 2, the lifetime values of the probe in micellar media are clearly more than those in water due to decrease in non-radiative decay rates. The radiative (k^r) and non-radiative (k^{nr}) decay rate constants (Table 2) are calculated using the following relations:

$$k^r = \Phi_F/\langle\tau\rangle \qquad k^{nr} = (1-\Phi_F)/\langle\tau\rangle \tag{3}$$

The increase in Φ_F and decay times and substantial decrease in k^{nr} in the micellar environment points toward the restricted motion of the probe inside the micellar

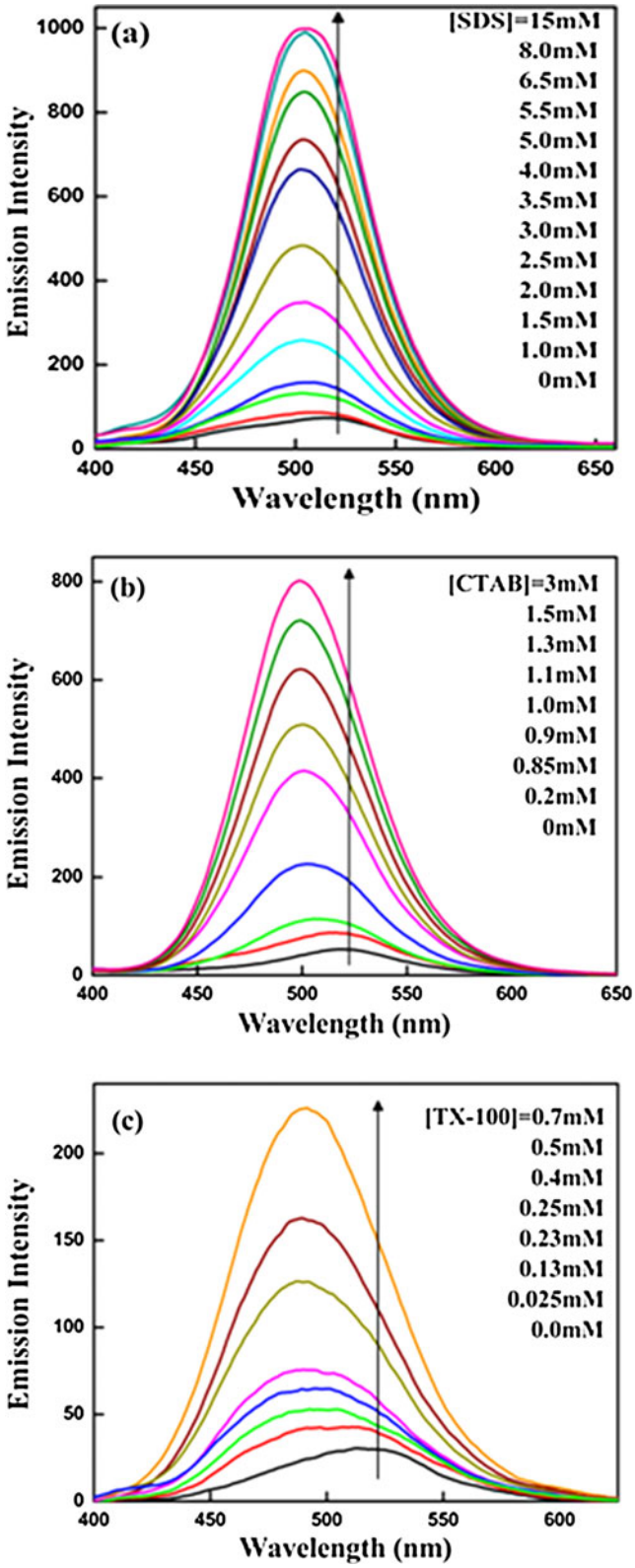

Fig. 2 Fluorescence emission spectra (λ_{ex}=350 nm) of EDMANA in micellar solution containing different concentrations of **a** SDS, **b** CTAB and **c** TX-100 at room temperature

cavities. According to Table 2, the fluorescence decay times increases in the order of SDS<CTAB<TX-100 and non-radiative rate constants as SDS>CTAB>TX-100.

Estimation of the Probe-Micelle Binding Constant

The enhancement and spectral shift of fluorescence intensity of EDMANA in micellar solution can be rationalized in terms of binding of the probe with the micelles. Binding constants of EDMANA with different micelles have been determined from the fluorescence intensity data following the method described by Almgren et al. [39]. According to this method, the binding constant (K_{eq}) can be obtained by changing the proportions of dissolved to 'free' solute from the following relationship

$$\frac{(I_\infty - I_0)}{(I_t - I_0)} = 1 + \frac{1}{K_{eq}[M]} \tag{4}$$

Where I_∞, I_0, I_t are the fluorescence intensities of the fluorophore under complete micellization, in the absence of micellization and in presence of intermediate amounts of surfactant respectively. [M] is related to the total concentration of the micelle and is calculated using following equation.

$$[M] = \frac{(S - CMC)}{N} \tag{5}$$

Where S represents the surfactant concentration and N is the aggregation number of the micelle. The N values used in the calculation of [M] are 62, 60 and 143 for SDS, CTAB and TX-100 respectively [40]. As seen in Fig. 4, a typical plot of $(I_\infty\text{-}I_0)/(I_t\text{–}I_0)$ versus 1/[M] following Eq. 4 shows linearity. The measured K_{eq} values are enlisted in Table 1. The K_{eq} values follow the order of the micelle SDS<CTAB<TX-100. In non-ionic micelle, the K_{eq} value is high due to the more stabilization of the CT probe in the micellar environment compared to other ionic micelles. Due to very thick (25 Å) palisade layer, most of the molecule may reside in this layer of the neutral TX-100 micelle whereas the fluorescent probe may reside in the interfacial region of SDS and CTAB as they have significantly thinner (6–10 Å) Stern layer. On the other hand, binding constant of EDMANA with CTAB is higher than SDS because the head group of SDS in the Stern layer is more hydrated than that of CTAB. From the K_{eq} values, the free energy changes ($\Delta G^0 = -RT\ln K_{eq}$) for the probe-micelle binding interaction in different micelles have been calculated at 293 K and the corresponding values are tabulated in Table 1. The free energy change clearly indicates that incorporation of probe inside the micelle cage is a spontaneous process.

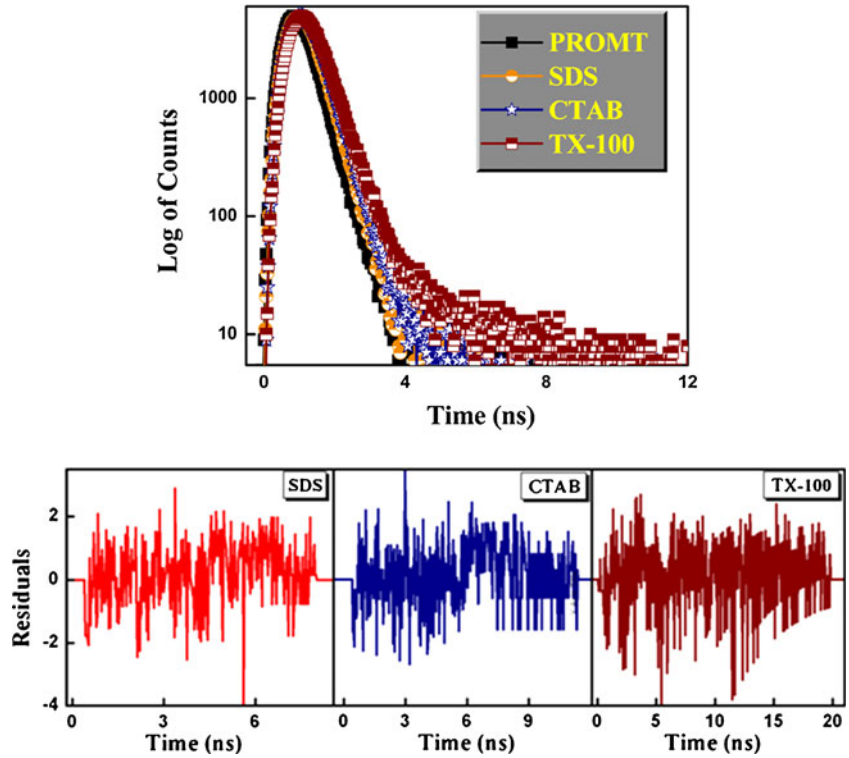

Fig. 3 Time resolved fluorescence decay of EDMANA in micellar media with λ_{ex}= 340 nm and λ_{em}=500 nm with the corresponding best fitted residuals.

Determination of Critical Micelle Concentration

Long chain surfactant molecules form micellar aggregates at the critical micelle concentration (CMC) and hence the microenvironments before and after CMC are quite different. Herein, EDMANA has been used to estimate the CMC values for the three surfactants and the typical plots of fluorescence intensity variation with surfactant concentration and the estimated CMC values are shown in Fig. 5 and are reported in Table 3. As can be seen in Table 3, the obtained CMC values using EDMANA as probe are in good agreement with the literature value [27].

Micropolarity Surrounding the Fluorophore in the Micellar Environment

As the determination of the polarity of the microenvironment in which the probe is located has great importance in biological systems, attention has been drawn to that direction using the $E_T(30)$ empirical solvatochromic scale [41]. Since the CT emission maxima shifts in the range ~17–30 nm in the micellar media and the CT emission is ~48 nm red shifted on changing the solvent from 1,4-dioxane to water, we can easily assume that the polarity around the probe in the micellar environment is intermediate between the polarities of water and 1,4-dioxane. A correlation is obtained from the plot of λ_{max}(em) of the probe in different composition of 1,4-dioxane-water mixture against $E_T(30)$ value. As shown in Fig. 6a, the emission maxima correlate linearly well with $E_T(30)$ values (R=0.988).

$$\lambda_{\max}(em) = 375.3 + 2.374E_T(30) \quad (6)$$

Substituting the λ_{max}(em) values for SDS, CTAB and TX-100 in Eq. 6 we have determined $E_T(30)$ values for three micelles and the values are 54.2, 51.7 and 49.2 kcal/mol respectively. Similarly, sharp changes occur in the correlation of the emission maxima of 1,4-dioxane-water

Table 2 Fluorescence decay parameters of EDMANA in different micellar media at room temperature (λ_{ex}=340 nm, λ_{em}=500 nm).

Medium	a_1	τ_1 (ns)	a_2	τ_2 (ns)	τ_{avg} (ns)	χ^2	k^r (10^9 s^{-1})	k^{nr} (10^{10} s^{-1})
SDS (20 mm)	1.0	0.162	–	–	0.162	1.18	0.185	0.599
CTAB (20 mM)	0.613	0.122	0.387	0.253	0.173	1.13	0.239	0.554
TX-100 (20 mM)	0.999	0.262	0.001	4.38	0.267	1.07	0.166	0.358

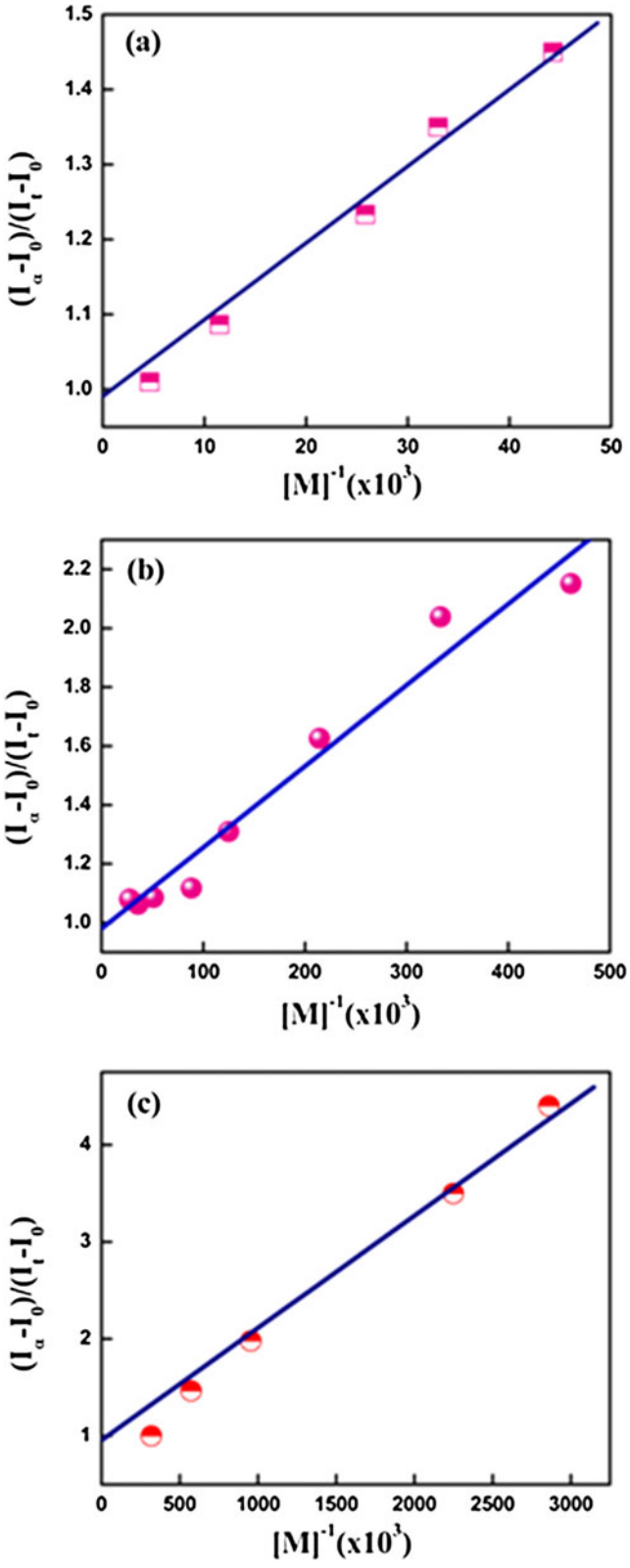

Fig. 4 Plot of $(I_\alpha - I_0)/(I_t - I_0)$ against $[M]^{-1}$ in **a** SDS, **b** CTAB and **c** TX-100

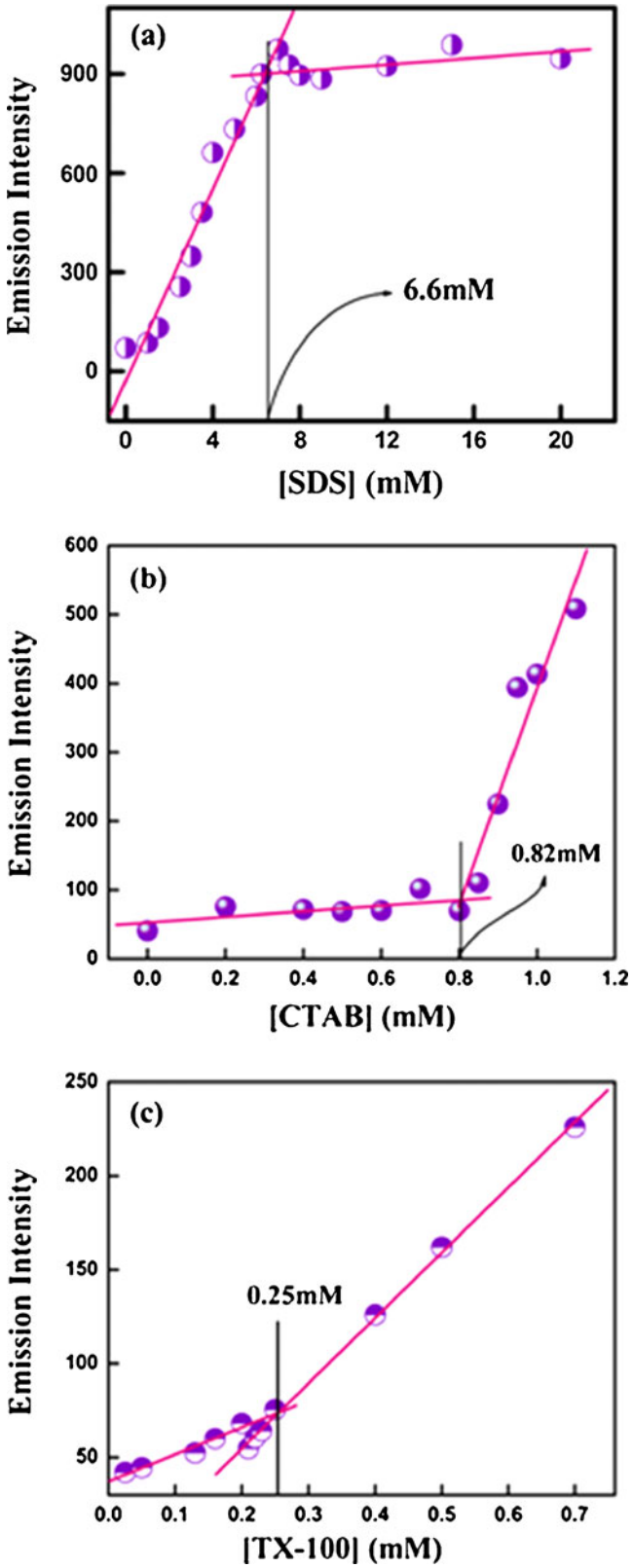

Fig. 5 Variation of fluorescence intensity of EDMANA as a function of concentration of **a** SDS, **b** CTAB and **c** TX-100

Table 3 CMC values of different micelles in absence and presence of urea using EDMANA as fluorescence probe

Medium	CMC (at 0 M urea)		CMC (at 6 M urea)	
	Measured value (mM)	Literature value (mM)	Measured value (mM)	Literature value (mM)
SDS	6.60	7.80 [27]	11.90	12.00 [32]
CTAB	0.82	0.94 [27]	1.53	1.36 [32]
TX-100	0.25	0.26 [27]	1.18	1.50 [33]

mixture with its dielectric constant as revealed in Fig. 6b. Table 4 gives the $E_T(30)$ and ε value of the micelles. From this study it is clear that the polarity of the microenvironment near the probe binding site is in the order of SDS>CTAB>TX-100 and hence CT emission of this molecular probe can be used for the measurement of micropolarity at the probe binding site. All the above observations indicate that the probe EDMANA resides in the interfacial region of micelle as the $E_T(30)$ and ε values of the probe in different micelles are higher than those of 1,4-dioxane ($E_T(30)$=36 kcal/mol, ε=2.2) but lower than those of water ($E_T(30)$=63 kcal/mol, ε=78.48).

Microviscosity of the Micellar Environment Around the Probe

As EDMANA undergoes twisted intramolecular charge transfer process in the excited state, any restrictions imposed on the excited state torsion of the fluorophore is expected to reflect in its emission behavior [31]. The plot of the fluorescence quantum yield data (Φ_F) versus viscosity (η) for the probe in water-glycerol mixtures shows that it is sensitive to viscosity (Fig. 6c) with a good linear relationship (R=0.996). Substituting the corresponding data for EDMANA in SDS, CTAB and TX-100 in Eq. 7

$$\Phi_F = 0.012 + 0.002\eta \quad (7)$$

the obtained values of viscosity are 7.672 cP, 11.075 cP and 11.890 cP, respectively, representing high viscous medium inside the micelles core.

CPCL Induced Fluorescence Quenching Study

To probe the location of the fluorophore in the micellar environment, we have studied the fluorescence quenching behavior of the encapsulated probe using cetyl pyridinium chloride (CPCL) as a quencher. The idea behind these

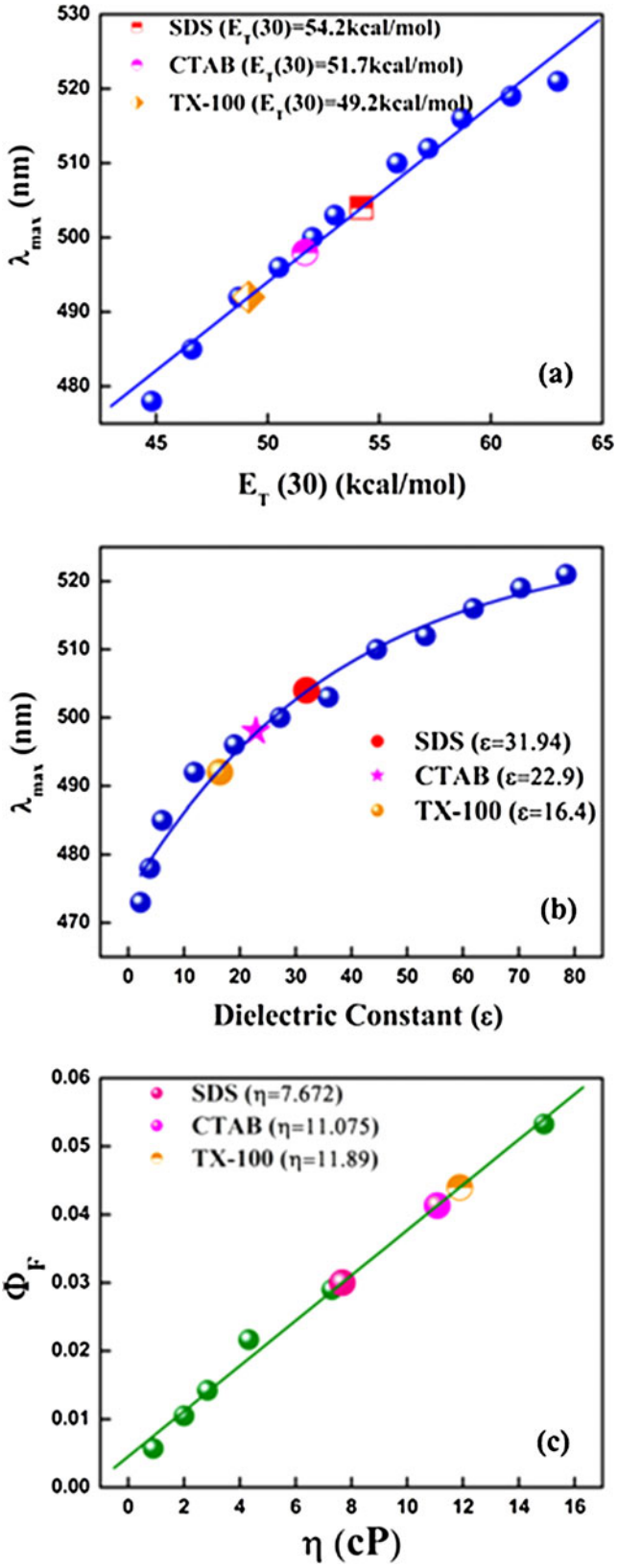

Fig. 6 Plots of the emission band maxima (λ_{max}(em)) of EDMANA versus **a** $E_T(30)$ and **b** dielectric constant (ε) on 1,4-dioxane-water mixed solvent. **c** Variation of fluorescence quantum yield (Φ_F) of EDMANA as a function of viscosity (η) of the glycerol water mixture (0%, 30%, 40%, 50%, 60%, 70% of glycerol). The corresponding parameters of SDS, CTAB and TX-100 are shown in the figures

Table 4 Dielectric constant (ε), Micropolarity $E_T(30)$, Microviscosity, and Quenching parameter of EDMANA in different micelles

Medium	$E_T(30)$ (kcal/mol)	Dielectric constant (ε)	η (cP)	K_{SV} (10^3 M^{-1})	k_q (10^{12} $M^{-1}s^{-1}$)
Water	63	78.48	–	–	–
SDS	54.2	31.94	7.672	0.61±0.06	4.01±0.39
CTAB	51.7	22.9	11.075	1.15±0.08	6.16±0.43
TX-100	49.2	16.4	11.890	1.07±0.08	4.21±0.31

measurements is that quencher with properties similar to the surfactant offers important advantages of ideal mixing over the more conventional quenchers like Cu^{2+}, I^- etc. The quencher, CPCL mixes ideally with the surfactants in the micelle and may enter into the Stern layer thereby causing fluorescence quenching. Here hydrophobic interaction plays the main role other than electrostatic forces. The fluorescence quenching was analyzed by the well known Stern-Volmer equation,

$$\frac{F_0}{F} = 1 + K_{SV}[Q] = 1 + k_q\tau[Q] \quad (8)$$

Where F_0 and F are the fluorescence intensities of the fluorophore in absence and presence of the quencher, respectively. K_{SV} and k_q are the Stern-Volmer constant and quenching rate constant of EDMANA respectively, τ is the lifetime of the probe in respective micellar microenvironment in absence of quencher and [Q] is the concentration of the quencher. As illustrated in Fig. 7, the plots of the relative fluorescence intensity versus quencher concentration are found to be linear. The obtained K_{SV} values as well as k_q values follow the order SDS<TX-100<CTAB (Table 4). The

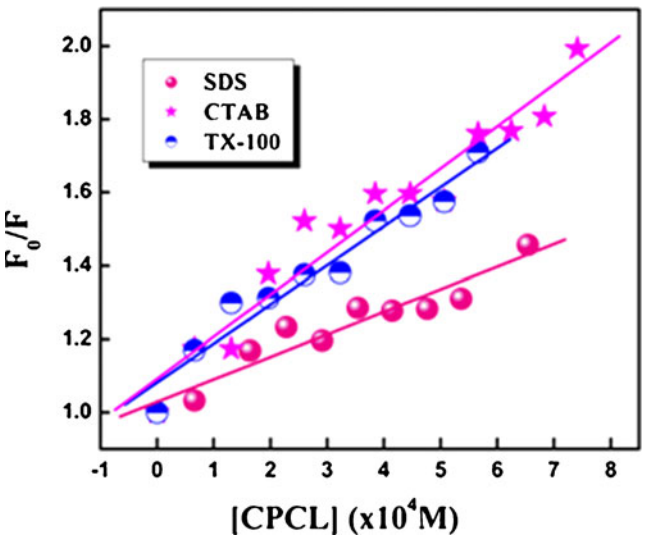

Fig. 7 Plot of relative fluorescence intensity of EDMANA in SDS (10 mM), CTAB (2 mM) and TX-100 (2 mM) as a function of the concentration of CPCL

quenching experiments clearly suggest that the fluorescing moiety is accessible to the quencher. The quencher resides at the Stern layer and has very low solubility near the micellar core region. If the fluorophore be located in the micellar core, there should be no appreciable fluorescence quenching due to unavailability of the quencher near the fluorophore. So EDMANA does not penetrate into the core of the micelle, rather it resides in the micelle-water interfacial region showing CPCL induced fluorescence quenching phenomenon.

In the excited state, the ICT state of EDMANA has calculated dipole moment of 13.67D [31]. When the charge is transferred from the donor to the acceptor part of the probe, the $–NMe_2$ group will carry more positive charge and the acceptor part will carry more negative charge. Since in SDS micelle, as seen in Scheme 2, the Stern layer contains negatively charged head groups and the Gouy-Chapman layer contains positively charged counter ions, the donor moiety try to reside in the Stern layer and the acceptor part in the Gouy-Chapman layer. In case of cationic micelle, CTAB, the electron donor $–NMe_2$ group resides in the Gouy-Chapman layer and the electron acceptor part will be located near the Stern layer. The possible orientations of EDMANA in ionic micelles have been pictured in Scheme 2. In case of TX-100, due to very thick palisade layer, the probe tends to reside in this layer of the micelle. It is further supported by the fact that $E_T(30)$ and ε value of EDMANA in TX-100 micelle are lower compared to that of ionic micelles (Table 4). So the fluorophore in TX-100 resides in less polar environment than SDS and CTAB.

Effect of Urea on Micelle-Probe Interaction

Urea, the well known denaturant of proteins, are very efficient as modifiers for the properties of aqueous solution. Since micelle formation arises as a result of a balance between hydrophobic and hydrophilic interactions, it is not surprising that urea has pronounced influence on the properties of micellar solution. There are some controversies about the mechanism on the action of urea on micelle. Does urea play as "water structure breaker" [42] or it displays some water molecules from the microenvironment of protein or micelle

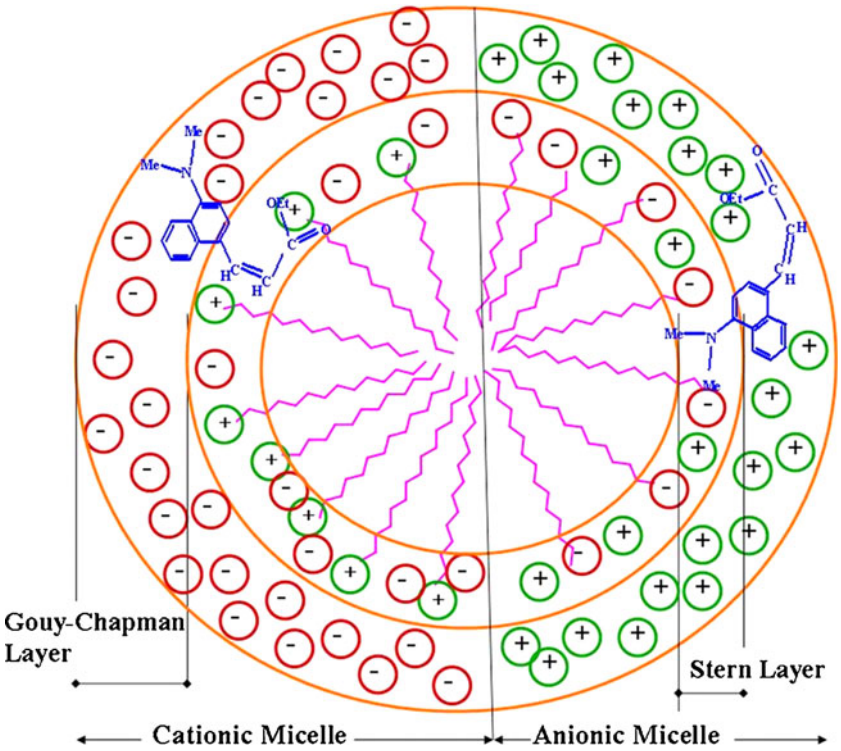

Scheme 2 Approximate location of the probe EDMANA in aqueous solution of cationic and anionic micelles

[43]? Although the former mechanism one is most accepted, but some theoretical and experimental reports contradict it thereby favoring the second opinion [44, 45]. The effect of urea on micelle is still a topic of debut and demands further investigation. Here, we have studied the effect of urea on the micelle bound EDMANA to gain further insight into photophysical modulation of micellar media in presence of chaotropes.

As shown in Fig. 8, addition of urea on micelle-bound probe decreases the fluorescence intensity suggesting that the fluorophore is discarded from the Stern layer to the bulk aqueous phase. This is consistent with other studies [44, 45] which indicates that urea changes solvation of hydrophobic group by displacing water molecules from surfaces. This perturbation of the nanocage environments desolvates some of the guest molecules and throws it out of the micellar media. The effect of urea in anionic micelle SDS is little bit different from those in CTAB and TX-100 micelle. It is clear from Fig. 8 that the changes in fluorescence intensity and fluorescence emission maxima remain more or less unaffected in SDS micelles whereas in case of CTAB and TX-100 sharp changes occur in both cases. We know that SDS with compact head group experiences smaller water penetration compared to the larger head group area such as CTAB and TX-100. For that reason, the fluorophore adjacent to the microheterogeneous environments are expelled more efficiently from the CTAB and TX-100 micelles than SDS micelle.

Effect of Urea on CMC of the Micelles

The change of CMC of the surfactant with a certain urea concentration has been followed here as it has already been reported that urea increases the CMC values of ionic and non-ionic surfactants [32, 33]. Figure 9 shows the variation of fluorescence intensity of EDMANA bound to SDS, CTAB and TX-100 micelles in 6 M urea. In the presence of this chaotrope, the slope change occurs at a concentration higher than that in the absence of urea thereby increasing the CMC values. The CMC value increases by a factor of ~2 for SDS and CTAB and ~5 for TX-100. The increase in CMC with 6 M urea concentration can be attributed to the ability of urea to weaken hydrophobic force responsible for the formation of the micelle assembly in the aqueous solution.

Conclusion

In this work, we have investigated photophysics of donor acceptor charge transfer molecule EDMANA inside the micellar nanocages and shown that this polarity sensitive probe serves as an excellent reporter for micellar micro-environments. The CT emission is found to be modulated much more by the media than the LE emission. The changes in viscosity and tight binding of the probe with micelles deactivate the non-radiative decay channels thereby

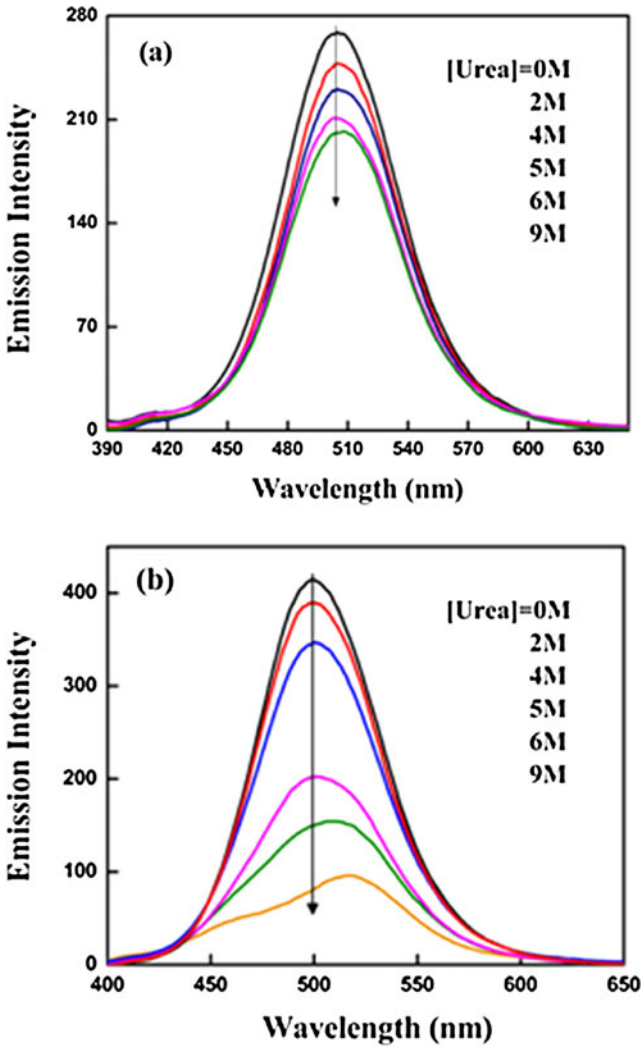

Fig. 8 Fluorescence spectra (λ_{ex}=350 nm) of micelle-bound EDMANA as a function of added urea in **a** 10 mM SDS and **b** 2 mM CTAB

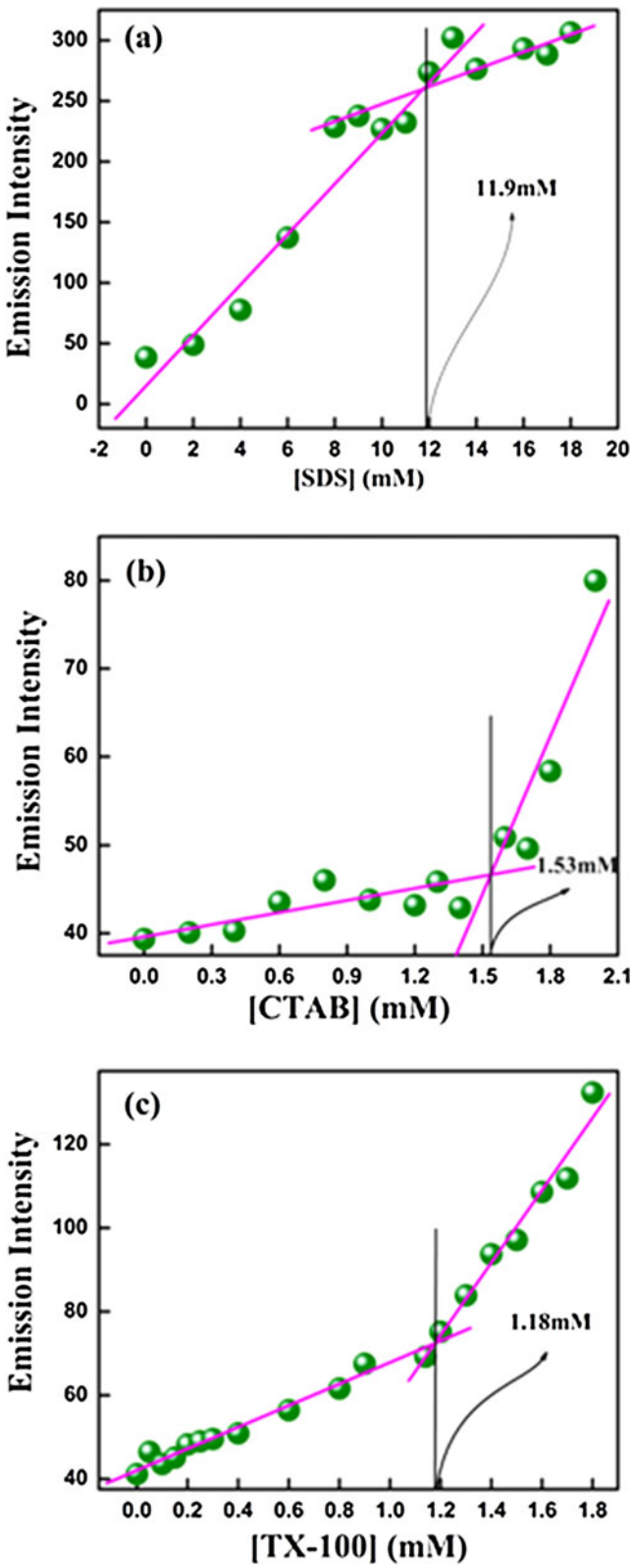

Fig. 9 Variation of fluorescence intensity of EDMANA in the presence of 6 M urea as a function of concentration of **a** SDS, **b** CTAB and **c** TX-100

increasing fluorescence intensity, quantum yield and influence other excited state properties. The micelle probe interaction and the location of the probe at the micelle-water interfacial region are ascertained by a variety of spectral parameters like $E_T(30)$, dielectric constants, microviscosity, binding constant, quenching parameters and non-radiative rate constant. All these studies infer that in anionic micelle the donor part of the target molecule resides in the Stern layer and the acceptor part remains bound in the Gouy-Chapman layer and the position of the probe in CTAB is just opposite to that in SDS. In case of TX-100, the probe EDMANA resides in the palisade layer due to its thickness (25 Å) thereby showing large extent of blue shifting and quantum yield value. The denaturant urea influences the binding interaction between probe and micelles. The increase of CMC of micelles in presence of urea by weaken of hydrophobic force has been studied by this CT fluorescence probe.

Acknowledgement AS and BKP thanks CSIR, New Delhi, for Senior Research Fellowship. We appreciate the cooperation received from Prof. T. Ganguly of IACS, Kolkata for his kind help in lifetime measurements. This work is supported by grants from DST, India (Project no. SR/S1/PC/26/2008) and CSIR, India (Project no. 01 (2161)07/EMR-II).

References

1. Lippert E, Luder W, Boos H (1962) Advances in molecular spectroscopy. Pergamon Press, Oxford, p 443
2. Rotkiewicz K, Grellman KH, Grabowski ZR (1973) Reinterpretation of the anomalous fluorescence of *p*-n, n-dimethylaminobenzonitrile. Chem Phys Lett 19:315–318
3. Kosower EM, Dodiuk H (1976) Multiple fluorescences. II. A new scheme for 4-(N, N-Dimethylamino)benzonitrile including proton transfer. J Am Chem Soc 98:924–929
4. Majumder D, Sen R, Bhattacharyya K, Bhattacharyya SP (1991) Twisted intramolecular charge transfer of p-(N, N-dimethylamino) benzonitrile: an approximate quantum mechanical study including solvation effects. J Phys Chem 95:4324–4329
5. Schenter GK, Duke CB (1991) Theory of photoinduced twisting dynamics in polar solvents: application to dimethylaminobenzonitrile in propanol at low temperatures. Chem Phys Lett 176:563–570
6. Marguet S, Mialocq JC, Millie P (1989) Intramolecular charge transfer and trans-cis isomerization of the DCM styrene dye in polar solvents. A CS INDO MRCI study. Chem Phys 160:265–279
7. LaFemina JP, Duke CB, Patton A (1987) Electronic structure and twisted intramolecular charge transfer in dimethylanilines. J Chem Phys 87:2151–2157
8. Hayashi S, Ando K, Kato S (1995) Reaction dynamics of charge-transfer state formation of 4-(N, N-Dimethylamino)benzonitrile in a methanol solution: theoretical analyses. J Phys Chem 99:955–964
9. Gorse A, Pesquer M (1995) Intramolecular charge transfer excited state relaxation processes in para-substituted N, N-dimethylaniline: a theoretical study including solvent effects. J Phys Chem 99:4039–4049
10. Grabowski ZR, Rotkiewicz K, Siemiarczuk A, Cowley DJ, Baumann W (1979) Twisted intramolecular charge transfer states (TICT). A new class of excited states with a full charge separation. Nouv J Chim 3:443–454
11. Rettig W (1986) Charge separation in excited states of decoupled systems—TICT compounds and implications regarding the development of new laser dyes and the primary process of vision and photosynthesis. Angew Chem Int Ed Engl 25:971–988
12. Van der Auweraer M, Grabowski ZR, Rettig W (1991) Molecular structure and the temperature-dependent radiative rates in Twisted Intramolecular Charge-Transfer and exciplex systems. J Phys Chem 95:2083–2092
13. Zachariasse KA, Grobys M, Tauer E (1997) Absence of dual fluorescence with 4-(dimethylamino) phenylacetylene. A comparison between experimental results and theoretical predictions. Chem Phys Lett 274:372–382
14. Sobolewski AL, Domcke W (1996) Promotion of intramolecular charge transfer in Dimethylamino derivatives: twisting versus acceptor-group rehybridization. Chem Phys Lett 259:119–127
15. Sun YP, Fox MA, Johnson KP (1992) Spectroscopic studies of p-(N, N-Dimethylamino)benzonitrile and ethyl p-(N, N-Dimethylamino)benzoate in supercritical trifluoromethane, carbon dioxide, and ethane. J Am Chem Soc 114:1187–1194
16. Schulte RD, Kauffman JF (1995) Fluorescence from the Twisted Intramolecular Charge Transfer Compound Bis(4,4′-Dimethylaminophenyl)sulfone in Ethanol/CO_2: A Probe of Local Solvent Composition. Appl Spectrosc 49:31–39
17. Cox GS, Huaptman PJ, Turro NJ (1984) Dialkylaminobenzonitriles as fluorescence polarity probes for aqueous solutions of cyclodextrins. Photochem Photobiol 39:597–601
18. Kim YH, Cho DW, Yoon M, Kim D (1996) Observation of hydrogen-bonding effects on twisted intramolecular charge transfer of p-(N, N-diethylamino)benzoic acid in aqueous cyclodextrin solutions. J Phys Chem 100:15670–15676
19. Al-Hassan KA (1994) The role of [alpha]-cyclodextrin cavity size on the fluorescence of 4-diethylaminobenzonitrile aqueous solution. Chem Phys Lett 227:527–532
20. Panja S, Chowdhury P, Chakravorty S (2003) Exploring the location and orientation of 4-(N, N-Dimethylamino) cinnamaldehyde in anionic, cationic and non-ionic micelles. Chem Phys Lett 368:654–662
21. Singh TS, Mitra S (2007) Fluorescence behavior of intramolecular charge transfer probe in anionic, cationic, and nonionic micelles. J Colloid Interface Sci 311:128–134
22. Ziang YB, Wang XJ, Jin MG, Lin LR (1999) The effect of micelle–water interface electric field on the intramolecular charge transfer within ionic micelle: dual fluorescence of sodium *p*-dialkylaminobenzoates in cetyltrimethylammonium micelles. J Photochem Photobiol A: Chem 126:125–133
23. Mallick A, Halder B, Maity S, Chattopadhyay N (2004) Constrained photophysics of 3-acetyl-4-oxo-6,7-dihydro-12H indolo-[2,3-a] quinolizine in micellar environments: a spectrofluorometric study. J Colloid Interface Sci 278:215–223
24. Sakthivel T, Florence AT (2003) Dendrimers & dendrons: facets of pharmaceutical nanotechnology. Drug Deliv Technol 3:73–78
25. Anwer K, Meaney C, Kao G, Hussain N, Shelvin R, Earls RM, Leonard P, Quezada A, Roland AP, Sullivan SM (2000) Cationic lipid-based delivery system for systemic cancer gene therapy. Cancer Gene Therapy 7:1156–1164
26. Rammurthy V (ed) (1991) Photochemistry in organized and constrained media. VCH, New York
27. Kalyanasundram K (1987) Photochemistry in microheterogeneous systems. Academic, New York
28. Mittal KL, Lindman B (eds) (1994) Surfactants in solution, vols. 1–3. Plenum, New York
29. Turro NJ, Grätzel M, Braun AM (1980) Photophysical and photochemical processes in micellar systems. Angew Chem Int Ed Engl 19:675–696
30. Menger FM (1979) The structure of micelles. Acc Chem Res 12:111–117
31. Singh RB, Mahanta S, Kar S, Guchhait N (2007) Spectroscopic study of excited state intramolecular charge transfer in ethyl ester of N, N′-Dimethylaminonaphthyl-(acrylic)-acid. Chem Phys 342:33–42
32. Dasgupta PK, Moulik SP (1989) Effects of urea and a nonionic surfactant on the micellization and counterion binding properties of cetyltrimethyl ammonium bromide and sodium dodecyl sulfate. Colloid Polymer Sci 267:246–254
33. Ruiz CC, Sánchez FG (1994) Effect of urea on aggregation behavior of triton X-100 micellar solutions: a photophysical study. J Colloid Interface Sci 165:110–115
34. Briganti P, Puvvada S, Blankschtein D (1991) Effect of urea on micellar properties of aqueous solutions of nonionic surfactants. J Phys Chem 95:8989–8995
35. Baglioni P, Dei L, Ferroni E, Kevan L (1991) Electron spin echo modulation and electron spin resonance studies of sodium dodecylsulfate and dodecyltrimethylammonium bromide micellar solutions: effect of urea addition. Progr Colloid Polym Sci 84:55–60
36. Mandal P, Kundu S, Misra T, Roy SK, Ganguly T (2007) Effects of liquid crystal environment on the spectroscopic and photophysical properties of well-known reacting systems 2,3-dimethylindole (DMI) and 9-cyanoanthracene (9CNA). J Phys Chem A 111:11480–11486

37. Velapoldi RA, Tønnesen HH (2004) Corrected emission spectra and quantum yields for a series of fluorescent compounds in the visible spectral region. J Fluores 14:465–471
38. Behera GB, Mishra BK, Behera PK, Panda M (1999) Fluorescent probes for structural and distance effect studies in micelles, reversed micelles and microemulsions. Adv Colloid Interface Sci 82:1–42
39. Almgren M, Griesser F, Thomas JK (1979) Dynamic and static aspects of solubilization of neutral arenes in ionic micellar solutions. J Am Chem Soc 101:279–291
40. Saroja G, Ramachandan B, Saha S, Samanta A (1999) The fluorescence response of a structurally modified 4-aminophthalimide derivative covalently attached to a fatty acid in homogeneous and micellar environments. J Phys Chem B 103:2906–2911
41. Reichardt G (1994) Solvatochromic dyes as solvent polarity indicators. Chem Rev 94:2319–2358
42. Finer EG, Franks F, Tait MJ (1972) Nuclear magnetic resonance studies of aqueous urea solutions. J Am Chem Soc 94:4424–4429
43. Roseman M, Jencks WP (1975) Interactions of urea and other polar compounds in water. J Am Chem Soc 97:631–640
44. Kuharski RA, Rossky PJ (1984) Molecular dynamics study of solvation in urea water solution. J Am Chem Soc 106:5786–5793
45. Mizutani Y, Kamogawa K, Nakanishi K (1989) Effect of urea on hydrophobic interaction: raman difference spectroscopy on the carbon-hydrogen stretching vibration of acetone and the carbon-nitrogen stretching vibration of urea. J Phys Chem 93:5650–5654